The Pittsburgh Sloan Digital Sky Survey Mg II Quasar Absorption-Line Survey Catalog

Anna M. Quider [1]
aquider@ast.cam.ac.uk
and

Daniel B. Nestor [2], David A. Turnshek [3],
Sandhya M. Rao [3], Eric M. Monier [4], Anja N. Weyant[3], and Joseph R. Busche[5]
[1] *Institute of Astronomy, Madingley Rd, Cambridge CB3 0HA, UK*
[2] *Department of Physics & Astronomy, University of California, Los Angeles, CA 90095*
[3] *Department of Physics & Astronomy, University of Pittsburgh, Pittsburgh, PA 15260*
[4] *Department of Physics, SUNY College at Brockport, NY 14420*
[5] *Department of Physics, Wheeling Jesuit University, Wheeling, WV 26003*

ABSTRACT

We present a catalog of intervening Mg II quasar absorption-line systems in the redshift interval $0.36 \leq z \leq 2.28$. The catalog was built from Sloan Digital Sky Survey Data Release Four (SDSS DR4) quasar spectra. Currently, the catalog contains $> 17,000$ measured Mg II doublets. We also present data on the $\sim 44,600$ quasar spectra which were searched to construct the catalog, including redshift and magnitude information, continuum-normalized spectra, and corresponding arrays of redshift-dependent minimum rest equivalent widths detectable at our confidence threshold. The catalog is available on the web. A careful second search of 500 random spectra indicated that, for every 100 spectra searched, approximately one significant Mg II system was accidentally rejected. Current plans to expand the catalog beyond DR4 quasars are discussed. Many Mg II absorbers are known to be associated with galaxies. Therefore, the combination of large size and well understood statistics makes this catalog ideal for precision studies of the low-ionization and neutral gas regions associated with galaxies at low to moderate redshift. An analysis of the statistics of Mg II absorbers using this catalog will be presented in a subsequent paper.

Subject headings: galaxies: ISM — quasars: absorption lines

1. Introduction

Quasar absorption line (QAL) surveys form the basis for selecting and studying large numbers of cosmologically-distant galaxies via their gas cross sections. Of particular usefulness among QALs is the Mg II$\lambda\lambda$2796,2803 resonance doublet. Mg^+ is a dominant ionization stage in gas having a large neutral hydrogen fraction, and the Mg II$\lambda\lambda$2796,2803 transitions have particularly strong oscillator strengths, making the doublet an excellent tracer of low-ionization and neutral gas. Additionally, in comparison to other UV absorption lines commonly found in quasar spectra, the relatively long rest wavelength of the doublet permits its identification with ground-based optical spectroscopy down to fairly low redshift ($z \gtrsim 0.14$; e.g., Nestor, Turnshek, & Rao 2006).

The utility of Mg II absorbers for the study of galaxies has prompted several QAL surveys in past decades. Initial studies were usually made at moderate spectral resolution and signal-to-noise

ratio, and this generally resulted in the detection of absorption systems with moderate to strong rest equivalent widths, $W_0^{\lambda 2796} \gtrsim 0.3$ Å. The first surveys (e.g., Weymann et al. 1979; Lanzetta, Turnshek, & Wolfe 1987; Tytler et al. 1987; Sargent, Steidel, & Boksenberg 1988; Caulet 1989) contained a few to a few dozen systems. The survey of Steidel & Sargent (1992), which identified more than 100 Mg II absorption systems, was the largest statistical sample of Mg II systems for more than a decade. Imaging surveys along quasar sightlines demonstrate that the bulk of the Mg II absorbers are associated with galaxies (e.g., Bergeron & Boissé 1991; Steidel, Dickinson, & Persson 1994; Kacprzak et al. 2010; Chen et al. 2010; Rao et al. 2011). Thus, the Mg II absorption-line catalogs have been used by various authors to study subsamples of systems with the aim of investigating the properties of the low-ionization and neutral gas regions associated with galaxies. These Mg II-based studies have the potential to reveal information on galactic halos/disks (e.g., Charlton & Churchill 1996), outflows induced by star formation and supernovae (e.g., Norman et al. 1996; Bond et al. 2001; Nestor et al. 2010), accreting protogalactic gas (Mo & Miralda-Escude 1996), merger-induced activity and tidal debris (e.g., Sargent & Steidel 1990; Maller et al. 2001; Kacprzak et al. 2007), dwarf galaxies (e.g., LeBrun et al. 1993), low surface brightness galaxies (e.g., Phillips, Disney, & Davis 1993), and even the extended environments of other quasars (e.g., Bowen et al. 2006). High-resolution spectroscopy is generally required to resolve the kinematic "component" structure of the absorbing gas; this component structure provides important detailed information on the velocity field of the gas associated with an absorbing galaxy (e.g., Churchill et al. 2000; Churchill & Vogt 2001; Steidel et al. 2002). It turns out that a significant fraction of strong Mg II systems ($W_0^{\lambda 2796} \geq 0.5$ Å) are damped Lyα (DLA) absorbers with neutral gas column densities $N_{HI} \geq 2 \times 10^{20}$ atoms cm^{-2}, and weaker Mg II systems are not DLAs (e.g., Rao, Turnshek, & Briggs 1995; Rao & Turnshek 2000; Rao, Turnshek, & Nestor 2006). Thus, Mg II-based surveys are particularly effective and important for preselecting systems to be used in DLA surveys at redshifts $z \lesssim 1.65$, when the Lyα line falls in the UV and is unobservable from the ground. For example, follow-up imaging of DLA galaxies shows that DLAs trace the neutral gas phase of a mixed population of galaxy types (e.g., Rao et al. 2003; Chen & Lanzetta 2003; Rao et al. 2011).

More recently, moderate resolution spectroscopy from the Sloan Digital Sky Survey (SDSS; York et al. 2000) has led to a huge increase in the number of quasar spectra available for QAL surveys. This has advanced the study of intervening absorption systems, moving sample sizes into the realm of high statistical significance. The survey of Nestor, Turnshek, & Rao (2005, hereafter NTR05) utilized ~ 3400 quasar spectra from the SDSS early data release (EDR). This present contribution is a continuation of the work begun in NTR05, and the reader is referred to NTR05 for additional details on the methods used here. From the spectra analyzed by NTR05, a statistical sample of over 1300 Mg II systems having $W_0^{\lambda 2796} \geq 0.3$Å was derived. In addition to providing a firm basis for the statistics of Mg II absorbers, that sample has also been used for follow-up studies, such as the first identification of a correlation between gas-phase metals and absorbing gas velocity spread (Nestor et al. 2003), an investigation of the mean spatial extent and photometric properties of Mg II absorbing galaxies (Zibetti et al. 2005), and an expanded investigation of DLAs at $z < 1.65$ (Rao et al. 2006). The Mg II EDR statistics have also been compared with Mg II statistics derived from a radio-selected sample of quasars in order to place an upper limit on the number of Mg II absorbers missed in optical surveys due to the dimming of background quasars by dust in the intervening absorbers (Ellison et al. 2004; Ellison & Lopez 2009). In the past few years, much larger Mg II absorber catalogs have been developed from subsequent data releases of the SDSS (e.g., Prochter, Prochaska, & Burles 2006; this contribution). Our present catalog has already been used to study the statistical properties of the absorbing gas and associated galaxies in order to take advantage of the high precision inherent in such large surveys. These studies include an expanded investigation of the correlation between metals and absorbing gas velocity spread (Turnshek et al. 2005), an expanded investigation of the mean spatial extent and photometric properties of the absorbing galaxies (Zibetti et al. 2007), investigations of the sightline velocity clustering

of the absorbers and the transverse spatial clustering of bright galaxies along the sightlines passing through them (Rimoldini 2007), an investigation of the dust extinction and gravitational lensing effects that the absorbers induce on background quasars (Ménard et al. 2008), and a sensitive search for emission associated with the absorbing galaxies (Ménard et al. 2011). In addition, follow-up imaging to search for galaxies associated with the rarest and strongest Mg II systems has taken place (Nestor et al. 2007, 2010).

In this paper we present the current state of our SDSS Mg II absorber catalog, which is presently complete through SDSS Data Release Four (DR4). As noted above, this contribution represents a continuation of the work presented by NTR05 in that we used the method of NTR05; however, we did not use their measurements of the EDR Mg II absorbers.[1] It contains $> 17,000$ absorbers in the redshift interval $0.36 \lesssim z \lesssim 2.28$ identified in $\sim 44,600$ SDSS quasar spectra. The catalog, along with other information (§4), is now publicly available at http://enki.phyast.pitt.edu/PittSDSSMgIIcat.php. Searches of more recent SDSS quasar spectra are underway, and in the future we hope to extend the catalog to include additional Mg II absorbers beyond DR4. However, future extensions will only be announced and made available on the Web site. The combination of size and well understood statistics makes the catalog ideal for (1) statistical studies of, for example, the properties and evolution of the low-ionization and neutral gas regions of galaxies, (2) identifying rare systems, which are readily identified only in very large surveys, and (3) selecting well-defined samples for follow-up studies. In a subsequent paper we will present and discuss the statistical properties of the absorbers in the present catalog (D. B. Nestor et al., in preparation).

2. Quasar Selection Criteria

The quasar spectra used to build the Mg II absorber catalog are a subset of the SDSS data releases through DR4. The searches for Mg II absorption doublets were generally performed on the initially released versions of the spectra. However, spectra have been re-extracted and re-calibrated in subsequent SDSS data releases (Adelman-McCarthy et al. 2008; Abazajian et al 2009). Therefore, for example, a quasar spectrum taken from DR7 may not be identical to the one we analyzed to form the catalog. However, since the nature of measuring an absorption-line equivalent width involves fitting a continuum and making a measurement over a small wavelength interval, the re-extraction and re-calibration of spectra will generally have no effect on the statistical properties of the absorbers in the catalog.

The quasar spectra to be searched for Mg II absorbers were isolated using an SQL query of the public SDSS DR4 database (available at http://cas.sdss.org/astrodr4/). All of the spectroscopic and photometric data in the SDSS are contained in two master tables: `SpecObjAll`, for spectroscopic data, and `PhotoObjAll`, for photometric data. The data in these two tables are organized into numerous "views" by imposing an array of selection criteria on the master tables. We used a `SpecPhoto` view to generate the quasar sample to be searched. The view we used was intended to eliminate all spectra of poor quality, sky spectra, duplicate observations (those spectra labeled as SECONDARY), and all data outside the primary DR4 survey area. In addition, `SpecPhoto` contains all of the spectroscopic information and the most accurate photometric information at the time of the data release (those observations labeled as BEST) for each included object.

We used four criteria to define the quasar sample: (1) a spectral classification of 3 or 4, which corresponds to `specClass = QSO` or `HIZ_QSO`, respectively, (2) $z > 0.36$ to ensure visibility of the Mg II $\lambda\lambda$2796,2803 doublet at the SDSS low wavelength limit of 3820 Å, (3) $zstatus > 1$ to eliminate missing or failed redshift measurements, and (4) $i < 20$ for the fiber magnitude. Incorporating these criteria into an SQL query of the `SpecPhoto` view yielded $\sim 44,600$ quasars. These quasars form the basis for the Mg II absorber catalog. The quasars that meet our redshift, magnitude, and zstatus selection criteria represent $\sim 72\%$ of all objects in SDSS DR4 which are spectroscopically classified as `QSO` or `HIZ_QSO`. Alternatively stated, $\sim 28\%$ of SDSS DR4 quasars were unsuitable for inclusion in the catalog because of emission red-

[1] The current version of the catalog does not include all EDR quasars. It only includes those quasars which meet our catalog's selection criteria (see §2).

shifts that were too low or poorly constrained, or magnitudes that were too faint for recording spectra of sufficient quality.

3. Construction of the Catalog

There were three main steps which led to the construction of the Mg II catalog: (1) automated processing of the quasar spectra, (2) visual inspection of the automatically identified Mg II candidate doublets to eliminate systems judged to be unreliable, and (3) measurement of the confirmed Mg II doublets. NTR05 developed this procedure and applied it to the SDSS EDR data. In this section, we briefly review these steps, referring the reader to NTR05 for more detail. When we generically refer to an absorption line's wavelength (λ_0), rest equivalent width (W_0), or error in rest equivalent width (σ_{W_0}), this applies to the particular line in question (e.g., see Table 1).

3.1. Automated Processing of Quasar Spectra

The automated processing of the quasar spectra is comprised of two distinct phases: the normalization of the spectra and identification of Mg II doublet candidates.

To maximize computation and storage efficiency, the data were abridged to exclude spectral regions not in the range to be searched for Mg II systems. This included the spectral regions shortward of the quasars' Lyα emission lines, in order to avoid the confusion and inaccuracy associated with searching in the Lyα forest, and longward of Mg II λ2800 broad emission lines, where intervening Mg II absorption would be absent. A combination of cubic splines and Gaussians was employed to fit the spectra, including the true continua and broad emission and broad absorption features. These continua fits, or pseudocontinua fits (i.e., continua that fit broad emission or absorption features and not just true continua), were used to normalize the spectral fluxes and flux uncertainties. The continuum-fitting process was successful for the vast majority ($\gg 99\%$) of spectra. The software only failed to derive satisfactory continua for a small number of quasars having rare spectra, such as extreme broad absorption-line (BAL) quasars; these spectra were excluded from the sample. Occasionally the automated software produced a poor fit in a localized spectral region. Such occurrences were very infrequent in comparison to the overall size of the survey, and always produced false candidates (rather than missing true systems) when present. These cases had no measurable effect on the overall properties of the catalog. In the uncommon circumstance (i.e., in $< 1\%$ of the cases) of a poor continuum fit being coincident with an Mg II absorption doublet, the fit was interactively re-fit to produce a satisfactory continuum before final equivalent width measurements were performed (see §3.3).

All normalized spectra were run though a routine that flags possible Mg II doublets. In order to isolate a sample of absorbers that were primarily intervening, systems with measured absorption redshifts within 3000 km s^{-1} of the SDSS quasar emission redshift were not included in the catalog. Therefore, biases that might arise due to overdensities of absorbers in quasar environments will be minimized or avoided in any statistical study based on the catalog. This same software also determines the λ2796 rest equivalent width detection limit, W_0^{lim} (see §3.3), as a function of redshift or observed wavelength, $(1+z) = \lambda_{obs}/2796.352$, for the range of Mg II redshifts corresponding to a searched spectral region. This W_0^{lim} information was recorded for each wavelength in each searched spectral region so that it could be integrated over all sightlines to determine the total number of redshift intervals surveyed as a function of W_0^{lim} and redshift (e.g., see Figure 8 in NTR05).

The Mg II doublet finding routine is conservative by design to ensure that all possible doublets are located in this initial step. A total of $\sim 44,600$ quasar spectra were searched for the Mg II absorption doublet. The conservative nature of our automated doublet finder led to a large number of flagged candidates: on average, more than two Mg II candidates were flagged for each quasar.

3.2. Visual Inspection of Candidate Mg II Doublets

All candidate Mg II doublets were individually inspected by eye to determine their validity. As the candidate-flagging routine was designed to be conservative, this resulted in the rejection of approximately 85% of all candidates during visual in-

spection.[2] The most common false positives were due to: (1) absorption in a BAL trough, (2) multiple identifications of a candidate Mg II doublet (this sometimes occurred within strong Mg II absorption profiles; we selected the apparent best absorption redshift and rejected redundant identifications), (3) non-Mg II absorption lines, or (4) coincidentally aligned noise spikes.

Consistent with previous QAL surveys (§1), our experience with the SDSS spectra has shown that isolated absorption features measured with a significance $\geq 5\sigma_{W_T}$ are what the eye determines to be confident detections. Here σ_{W_T} is the theoretical error in rest equivalent width used to calculate the detectability limit, W_0^{lim}, of an Mg II doublet (see §3.3). When combined with additional information, such as the confident detection of a doublet partner, significances $\geq 3\sigma_{W_T}$ tend to be consistent with confident-by-eye detections. Candidate doublets identified with significances close to these thresholds would often be difficult to categorize as real or spurious based on quick visual inspection. Such candidates were generally retained at this stage by default. However, after final measurements were available (see §3.3), we used visual inspection to reject suspicious candidates. This included candidates with doublet ratios significantly different from the physically-allowed range of 1.0 $\leq W_0^{\lambda 2796}/W_0^{\lambda 2803} \leq$ 2.0. We also examined each spectrum to assess the possibility that a candidate Mg II system was flagged due to the presence of a QAL system at another redshift, and candidates which were not convincingly Mg II were rejected.

3.3. Measurements of Mg II Doublets

The reported measurements of the redshifts and rest equivalent widths of all accepted systems were finalized interactively when necessary. A pair of Gaussian line profiles separated in wavelength by the redshifted doublet separation was fitted to each accepted candidate's profile. The location of these fitted profiles defined the observed redshift and was used to perform an optimal extraction (see NTR05) of each line's rest equivalent width, W_0, and its associated error, σ_{W_0}. This is the optimal procedure when the observed profile is well described by the chosen function. We draw particular attention to Equations (1) and (2) from NTR05:

$$(1+z)\,W_0 = \frac{\sum_i P(\lambda_i - \lambda_0)\,(1-f_i)}{\sum_i P^2(\lambda_i - \lambda_0)}\,\Delta\lambda, \quad (1)$$

$$(1+z)\,\sigma_{W_0} = \frac{\sqrt{\sum_i P^2(\lambda_i - \lambda_0)\,\sigma_{f_i}^2}}{\sum_i P^2(\lambda_i - \lambda_0)}\,\Delta\lambda, \quad (2)$$

where $P(\lambda_i - \lambda_0)$, λ_i, f_i, and σ_{f_i} represent the line profile centered at λ_0, the wavelength, the normalized flux, and flux uncertainty as a function of pixel. The sum is performed over an integer number of pixels that cover at least ± 3 characteristic Gaussian widths. For systems with clearly saturated or resolved profiles, two pairs of Gaussians were used to fit the absorption system, and this proved to be almost always successful at accurately reproducing the observed profiles. In these cases the reported redshift is the rest-equivalent-width-weighted redshift. For weaker and/or unresolved systems, the additional degrees of freedom afforded by a double-Gaussian did not generally give different values for $W_0^{\lambda 2796}$ and $W_0^{\lambda 2803}$. In over 95% of the cases, doublet members were fit with single-Gaussian profiles. Upon careful inspection of the systems retained in the catalog after measurement, it was found that systems stronger than $W_0^{\lambda 2796} \gtrsim 3$ Å frequently had their strengths slightly ($< 1\sigma_{W_0}$) but systematically overestimated when using a single-Gaussian profile fit. Therefore, the ~ 700 strongest systems were re-inspected and re-measured using double Gaussians when appropriate. The centroids of each Gaussian were left free during the fit.

Consistent with experience (§3.2), the values for the λ2796 rest equivalent width detection limit, W_0^{lim}, as a function of redshift or observed wavelength, $(1+z) = \lambda_{obs}/2796.352$, were calculated by requiring $W_0^{\lambda 2796} \geq 5\sigma_{W_T}$ and $W_0^{\lambda 2803} \geq 3\sigma_{W_T}$. Thus, to compute W_0^{lim} for each spectrum we did the following. We started by determining the 1σ rest equivalent width error, σ_{W_0} (Equation (2)), for a theoretical, unresolved line near the location of each doublet member and set $\sigma_{W_T} = \sigma_{W_0}$. We then took the value of W_0^{lim} to be the larger of five times this error ($5\sigma_{W_T}$) at the location of the λ2796 line or six times this error ($2 \times 3\sigma_{W_T}$) at the location of the λ2803 line. The factor of two avoids introducing a detection bias caused by the

[2] The high rate of visual rejection may have unfortunately resulted in the accidental rejection of some clearly significant candidates (see §4.2).

Mg II doublet ratio, which has a theoretical range of approximately 1.0 (completely saturated) to 2.0 (completely unsaturated). Systems with measured $W_0^{\lambda 2796} < W_0^{lim}$ were excluded from the catalog. This eliminated the vast majority of suspicious systems that were not rejected during visual inspection. At this point, $\sim 17,000$ Mg II doublets were considered real and successfully measured. Whenever possible, systems close in redshift were measured as separate systems. It is important to note that the redshift difference for which this was possible was not constant, because it depended on both redshift and the widths of the features, and therefore on $W_0^{\lambda 2796}$ and $W_0^{\lambda 2803}$. We retained such systems as separate in the catalog and note that they can always be combined *ex post facto* for statistical purposes, when necessary. This is a deviation from the policy of NTR05, where systems with separations less than 500 km s^{-1} were always measured as a single system.

3.4. Measurements of Adjacent Mn II, Fe II, and Mg I Absorption Lines in Cataloged Mg II Systems

In addition to the measurements of Mg II $\lambda\lambda$2796,2803 doublets, we also made rest equivalent width measurements at the predicted locations of six additional absorption lines (Fe II $\lambda\lambda$2586, 2600, Mn II $\lambda\lambda$2576, 2594, 2606, and Mg I λ2852) for all of the systems in the catalog, when possible. Since these lines are not too far displaced from the Mg II doublet, it was usually possible to make measurements at their predicted locations. There are many significant detections. For example, for Mg II systems in the redshift interval $0.36 \leq z \leq 2.28$ in SDSS spectra, the Mn II λ2576 transition is usually covered when $z > 0.48$ and the Mg I λ2852 transition is usually covered when $z < 2.22$. Including non-detections caused by lack of coverage, the 2σ and 3σ detection fractions for these six absorption transitions are as follows: Fe II λ2586 (53.7% and 43.6%), Fe II λ2600 (73.5% and 64.1%), Mn II λ2576 (10.9% and 4.9%), Mn II λ2594 (8.1% and 3.3%), Mn II λ2606 (7.0% and 2.7%), and Mg I λ2852 (40.6% and 27.9%).

One motivation for making these additional measurements is to facilitate future use of this catalog to identify candidate DLA systems. For example, as discussed by Rao et al. (2006), it appears that measurements of Fe II λ2600, Mg II λ2796, and Mg I λ2852 can be used together to isolate a subset of Mg II systems that will contain a complete sample of DLA systems, but with a higher DLA fraction than previously achieved. For example, follow-up UV spectroscopy to measure N_{HI} in a properly selected subset of Mg II systems (see Rao et al. 2006) indicates that the sample will be complete and $\sim 42\%$ will be DLAs.

Figure 1 shows two regions of a spectrum containing one of the Mg II absorption-line systems in the catalog. The absorption system is in the spectrum of quasar SDSS J085244.74+343540.4 ($z_{em} = 1.655$) and the absorption redshift is $z = 1.310$. The figure shows the Mg II doublet and the six additional metal-line absorption transitions that have been measured for this system. Table 1 presents the metal-line measurements for this system as an example of information that may be found in the catalog.

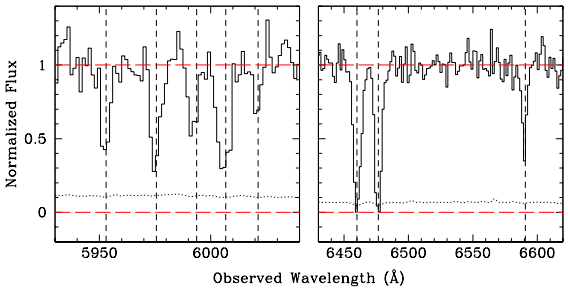

Fig. 1.— Two regions of the normalized spectrum of SDSS quasar J085244.74+343540.4 showing eight metal absorption-line transitions at $z = 1.3102$ (Mn II λ2576, Fe II λ2586, Mn II λ2594, Fe II λ2600, Mn II λ2606, Mg II $\lambda\lambda$2796,2803, and Mg I λ2852). The lower dotted curve is the 1σ error in normalized flux.

4. The Catalog Characteristics

4.1. The Catalog Format

The Pittsburgh SDSS Mg II Quasar Absorption-Line Survey Catalog is available for public use at http://enki.phyast.pitt.edu/PittSDSSMgIIcat.php.

It includes information about the quasars that were searched for Mg II doublets, the measurements of the Mg II doublets (§3.3), the measurements of up to six additional metal absorption lines (§3.4), and the quasar spectral files in text format. Values of W_0^{lim} (§3.3) have been merged with the quasar spectral files, so the available quasar spectral files contain flux, flux uncertainty, pseudo-continuum fit, and W_0^{lim}, all as a function of wavelength. The quasar properties in Table 2 are available for each quasar that was searched for Mg II. Table 2 is drawn from DR4, and we refer the reader to http://www.sdss.org/dr4 for further explanation of the values given in the table.

In summary, quasar spectra files and DR4 quasar properties are made available for $\sim 44,600$ quasars, and absorption system information is available for $> 17,000$ Mg II doublets.

4.2. Missed Systems

We have attempted to quantify our incidence of missed Mg II absorption doublets which are real, clearly significant, and located within our searched quasar sample. There are two possible steps during the construction of the catalog where one might think that an Mg II system could be missed or lost: (1) the automated Mg II identification routine and (2) the interactive inspection and/or measurement of a candidate Mg II system which often results in removing a system for the reasons given in §3.2 and §3.3. As the Mg II identification software has been robustly tested and conservatively written (see NTR05), we are confident that the first possibility is an exceedingly small source of missed Mg II absorbers when compared to the second possibility, which includes the potential for human error.

To quantify our incidence of missed Mg II absorption systems, we randomly selected 500 quasars from our catalog. Two of us (A.M.Q and D.B.N) then visually inspected 200 separate spectra and 100 common spectra (for a total of 500 spectra) to search for Mg II absorbers. As explained in §3.2, our formal detection/rejection threshold is such that the human eye seems to be generally capable of identifying Mg II absorbers to slightly better than the sensitivity limit (W_0^{lim}) adopted for the construction of the catalog. Therefore, manually re-inspecting the spectra for Mg II absorption doublets in a slow and careful manner allows us to account not only for software errors, but also human errors made during the initial laborious process of manually accepting/rejecting candidates from the extremely large master list. In the entire sample of 500 spectra, we discovered five significant missed systems with $W_0^{\lambda 2796} - W_0^{lim} > \sigma_{W_0}$. Therefore, we conclude that human error caused the rejection of some systems. We estimate that for every 100 searched spectra approximately one Mg II absorber unambiguously above our detection threshold has been missed. This is a systematic human error that appears not to be correlated with any Mg II system property.

4.3. Quasar Properties

Figure 2 shows the distribution of SDSS emission redshifts for all quasars in the catalog along with the distribution of absorption redshifts for all Mg II systems in the catalog. The distribution of emission redshifts is similar to the one derived from the DR5 quasar catalog (Schneider et al. 2007).[3] Schneider et al. (2007) note that the dips in the emission redshift distribution near $z = 2.7$ and $z = 3.5$ are due to the SDSS quasar selection algorithm. Figure 3 shows the SDSS i magnitude (left panel) and g magnitude (right panel) distributions for all quasars in the catalog (red dotted line) and for those quasars with at least one intervening Mg II absorption system (black solid line). The i magnitude distribution is similar to the one published by Schneider et al. (2007) for DR5 quasars. The bottom panels of Figure 3 show the corresponding fractions of quasars with one or more Mg II systems as a function of magnitude, without regard to quasar redshift. As expected, the brighter quasars have a higher probability of exhibiting Mg II absorption since the high signal-to-noise ratio of their spectra permits the detection of weaker Mg II systems, which have a higher incidence than stronger systems (e.g., NTR05).

4.4. Mg II Absorber Properties

A thorough treatment of the Mg II absorber statistics from the catalog will be presented in a subsequent paper (D. B. Nestor et al., in preparation). Here, we present the raw properties of

[3] A DR4 quasar catalog was not published.

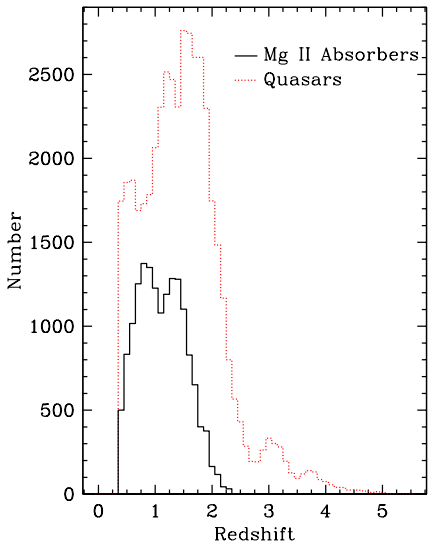

Fig. 2.— Emission redshift distribution for all quasars in the catalog (red dotted line) and the absorption redshift distribution for all Mg II systems in the catalog (black solid line). The redshift bin width for both distributions is 0.1. The emission redshift range of the quasars in the catalog is constrained by the criteria given in §2. The absorption redshift range of the Mg II systems is determined by the wavelength coverage of SDSS spectra, namely $0.36 \lesssim z \lesssim 2.28$. The drop in the number of absorption systems near $z \approx 1.1$ is due to a decrease in SDSS spectrograph sensitivity in the transition region from the blue-side to red-side cameras.

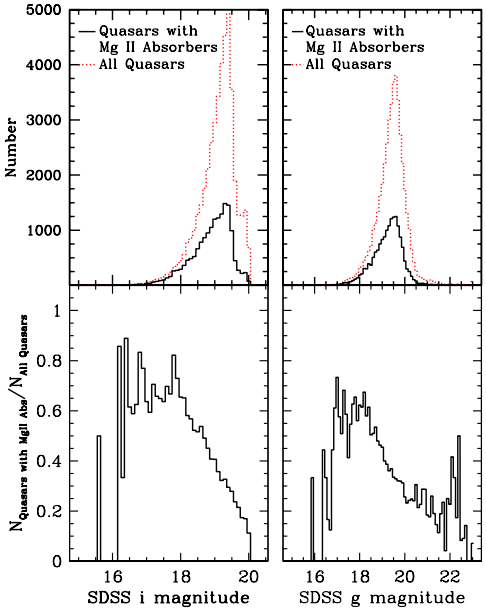

Fig. 3.— Top panels show the i (left) and g (right) magnitude distributions for all quasars in the catalog (red dotted line) and for those quasars with one or more Mg II absorbers (black solid line). The magnitude bin width is 0.1. The bottom panels show the corresponding fractions of quasars with one or more Mg II systems as a function of magnitude, without regard to quasar redshift. As expected, the brighter quasars have a higher probability of exhibiting Mg II absorption since the high S/N of their spectra permits the detection of weaker Mg II systems, which have a higher incidence than stronger systems.

the Mg II doublets in the catalog to illustrate the properties of the catalog itself.

Returning to Figure 2, the black histogram shows the distribution of absorber redshifts for Mg II doublets in the catalog. The redshift distribution of the Mg II absorbers is constrained to lie between $0.36 \lesssim z \lesssim 2.28$ because of the wavelength coverage of the SDSS spectrograph. As mentioned in NTR05, the dip at $z \approx 1.1$ is due to the ubiquitous decrease in signal-to-noise ratio at the wavelength corresponding to the split between the blue-side and red-side cameras by the dichroic. The black histograms in the top panels of Figure 3 show the distribution of i and g magnitudes for quasars having at least one Mg II absorber in its spectrum. As noted in §4.3, the bottom panels indicate that a higher fraction of Mg II systems have been detected in brighter quasars. This is due to the fact that the higher signal-to-noise ratios of the brighter quasars permit the detection of weaker Mg II systems, which have a higher incidence than stronger Mg II systems.

The observed $W_0^{\lambda 2796}$ distribution is presented in Figure 4. Nearly 50% of the absorbers have 0.6 Å $< W_0^{\lambda 2796} < 1.2$ Å. We identify $\sim 10,000$ Mg II absorbers with $W_0^{\lambda 2796} > 1.0$ Å. For comparison, Prochter et al. (2006) compiled 7,421 Mg II absorbers with $W_0^{\lambda 2796} > 1.0$ Å in their SDSS DR3 catalog. A large fraction of the absorbers in

our catalog have high rest equivalent width, with ∼16% having $W_0^{\lambda 2796} > 2.0$ Å.

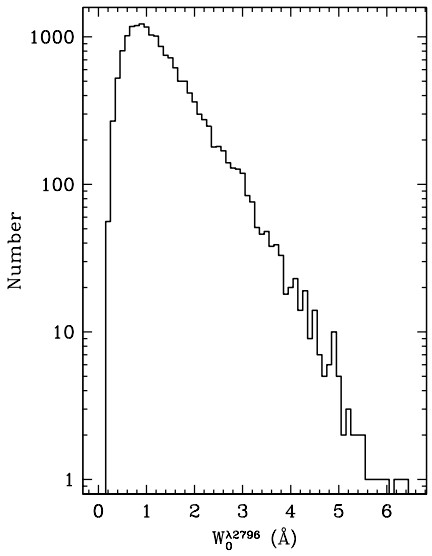

Fig. 4.— Observed λ2796 rest equivalent width, $W_0^{\lambda 2796}$, distribution for the Mg II absorbers in the catalog. The bin width is 0.1 Å.

Figures 5 and 6 show the measured relationship between $W_0^{\lambda 2796}$ and $W_0^{\lambda 2803}$. The diagonal lines in Figure 5 represent the theoretical limits for completely saturated ($W_0^{\lambda 2796}/W_0^{\lambda 2803} = 1.0$) and unsaturated ($W_0^{\lambda 2796}/W_0^{\lambda 2803} = 2.0$) absorption. The error bars along the horizontal axis represent the average measured σ_{W_0} for various rest equivalent width regions. Figure 6 illustrates the relationship between the doublet ratio and the value of $W_0^{\lambda 2796}$.

The vast majority of the Mg II absorbers in the catalog have doublet ratios that lie within the theoretical limits, and deviations from these limits can be attributed to noise and line blending. In some instances, for example, systems that are clearly real, exhibiting high-significance metal lines from other species at the same absorption redshift, will have poorly measured $W_0^{\lambda 2803}$ values due to contamination from a line in another absorption system. Such systems may have measured doublet ratios well outside of the theoretical range. Most of our effort has been given to obtaining the best possible measurements of $W_0^{\lambda 2796}$ in identified systems. Therefore, these values can generally be used with more confidence. Of course,

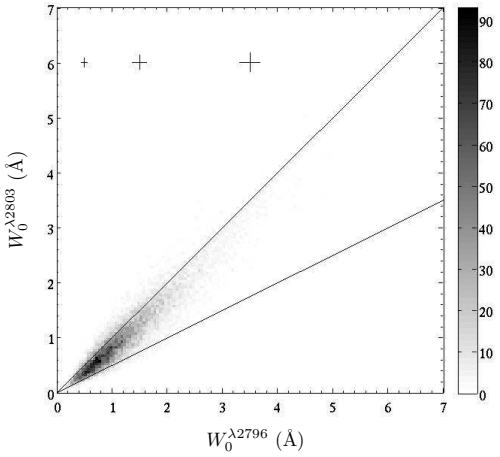

Fig. 5.— Plot of $W_0^{\lambda 2796}$ vs. $W_0^{\lambda 2803}$ for absorbers in the catalog is shown. The two diagonal lines represent the theoretical boundaries for the Mg II doublet ratios in a hypothetical error-free data set (i.e., $1 \leq W_0^{\lambda 2796} \setminus W_0^{\lambda 2803} \leq 2$). The vast majority of doublets in the catalog have doublet ratios that fall within the theoretical boundaries. Those that fall outside the theoretical boundaries can be attributed to errors associated with noise and/or line blending. The crosses in the upper left corner represent the average $\pm 1\sigma_{W_0}$ errors in the $W_0^{\lambda 2796}$ and $W_0^{\lambda 2803}$ measurements for $W_0^{\lambda 2796} = W_0^{\lambda 2803} \approx 0.5$ Å, 1.5 Å, and 3.5 Å, respectively. The gray-scale bar on the right-hand side provides information on the frequency distribution of doublet ratios.

we also attempt to measure an accurate value for $W_0^{\lambda 2803}$, but less effort and no testing has been devoted to determining possible problems with these measurements. Therefore, more caution should be exercised if the desire is to use the $W_0^{\lambda 2803}$ values in high-precision studies.

5. Summary

We present the Pittsburgh SDSS Mg II Quasar Absorption-Line Survey Catalog – a well-characterized catalog of Mg II absorption doublets found in the spectra of quasars up through SDSS DR4, along with supporting information. We have combined

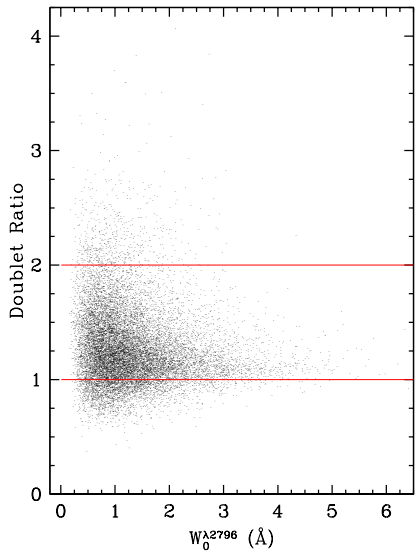

Fig. 6.— Plot of $W_0^{\lambda 2796}$/ $W_0^{\lambda 2803}$ vs. $W_0^{\lambda 2796}$ for the Mg II absorption doublets in the catalog. This is a different rendering of the same data shown in Figure 5.

automated and manual techniques to search the spectra of $\sim 44,600$ quasars to arrive at a catalog of $> 17,000$ Mg II $\lambda\lambda$2796,2803 absorption doublets which we now make available for public use. The available information includes the Mg II absorber catalog itself, with measurements of the absorbers and associated errors, measurements of up to six nearby metal absorption lines (Mn II, Fe II, and Mg I), and information on the quasar catalog which was searched, including wavelength-dependent spectral files (flux, flux uncertainty, pseudo-continuum fit, and λ2796 rest equivalent width detection limit) for each quasar. The results contain the information necessary for statistical studies. We estimate that for every 100 searched spectra approximately one Mg II absorber unambiguously above our detection threshold has been missed. A complete analysis of the statistics of the catalog will be given in a subsequent paper (D. B. Nestor et al., in preparation).

We make the catalog available to the community with the hope that its very large size and documented statistical characteristics will lead to future innovative investigations at low to moderate redshift. Any future extensions to the catalog, which would include data beyond SDSS DR4, will only be announced and made available at the catalog's Web site http://enki.phyast.pitt.edu/PittSDSSMgIIcat.php. Please email queries regarding the catalog to mgiicat@pitt.edu.

AMQ is supported by a Marshall Scholarship and a National Science Foundation Graduate Research Fellowship. DAT and SMR acknowledge support from NSF grant AST-0307743. AMQ and ANW acknowledge REU support from NSF grants AST-0307743 and PHY-0244105. DBN acknowledges early support from Zaccheus Daniel and Andrew Mellon pre-doctoral Fellowships at the University of Pittsburgh and support from the STFC-funded Galaxy Formation and Evolution programme at the Cambridge Institute of Astronomy.

We thank Eric Furst and Daniel Owen for their assistance with the visual inspection of candidate Mg II doublets. The involvement of these undergraduate students was made possible by REU support from NSF grants AST-0307743 and PHY-0244105.

We are grateful to the anonymous referee for helpful comments. We thank members of the SDSS collaboration who made the project a success.

Funding for the creation and distribution of the SDSS Archive has been provided by the Alfred P. Sloan Foundation, Participating Institutions, NASA, NSF, DOE, the Japanese Monbukagakusho, and the Max-Planck Society. The SDSS Web site is http://www.sdss.org. The SDSS is managed by the Astrophysical Research Consortium for the Participating Institutions: the American Museum of Natural History, Astrophysical Institute Potsdam, University of Basel, Cambridge University, Case Western Reserve University, University of Chicago, Drexel University, Fermilab, the Institute for Advanced Study, the Japan Participation Group, Johns Hopkins University, the Joint Institute for Nuclear Astrophysics, the Kavli Institute for Particle Astrophysics and Cosmology, the Korean Scientist Group, the Chinese Academy of Sciences (LAMOST), Los Alamos National Laboratory, the Max-Planck-Institute for Astronomy (MPIA), the Max-Planck-Institute for Astrophysics (MPA), New Mexico State University, Ohio State University, University of Pitts-

burgh, University of Portsmouth, Princeton University, the United States Naval Observatory, and University of Washington

REFERENCES

Abazajian, K.N., et al. 2009, ApJS, 182, 543

Adelman-McCarthy, J.K., et al. 2008, ApJS, 175, 297

Bergeron, J., & Boissé, P. 1991, A&A, 243, 344

Bond, N.A., Churchill, C.W., Charlton, J.C., & Vogt, S.S. 2001, ApJ, 562, 641

Bowen, D.V., et al. 2006, ApJ, 645, L105

Caulet, A. 1989, ApJ, 340, 90

Charlton, J.C., & Churchill, C.W. 1996, ApJ, 465, 631

Chen, H.-W., & Lanzetta, K.M. 2003, ApJ, 597, 706

Chen, H.-W., Helsby, J.E., Gauthier, J.-R., Shectman, S.A., Thompson, I.B., & Tinker, J.L. 2010, ApJ, 714, 1521

Churchill, C.W., Mellon, R.R., Charlton, J.C., Jannuzi, B.T., Krihakos, S., Steidel, C.C., & Schneider, D.P. 2000, ApJ, 543, 577

Churchill, C.W., & Vogt, S.S. 2001, AJ, 122, 679

Ellison, S.L., Churchill, C.W., Rix, S.A., & Pettini, M. 2004, ApJ, 615, 118

Ellison, S.L., & Lopez, S. 2009, MNRAS, 397, 467

Kacprzak, G.G., Churchill, C.W., Steidel, C.C., Murphy, M.T., & Evans, J.L. 2007, ApJ, 662, 909

Kacprzak, G.G., Churchill, C.W., Ceverion, D., Steidel, C.C., Klypin, A., & Murphy, M.T. 2010, ApJ, 711, 533

Lanzetta, K.M., Turnshek, D.A., & Wolfe, A.M. 1987, ApJ, 322, 739

LeBrun, V., Bergeron, J., Boisse, P., & Christian, C. 1993, A&A, 279, 33

Maller, A., Prochaska, J.X., Somerville, R.S, & Primack, J.R. 2001, MNRAS, 326, 1475

Ménard, B., Nestor, D., Turnshek, D., Quider, A., Richards, G., Chelouche, D., & Rao, S. 2008, MNRAS, 385, 1053

Ménard, B., Wild, V., Nestor, D. B., Quider, A., Rao, S., & Turnshek, D. A. 2011, MNRAS, in press

Mo, H.J., & Miralda-Escude, J. 1996, ApJ, 469, 58

Nestor, D.B., Rao, S.M., Turnshek, D.A., & Vanden Berk, D. 2003, ApJ, 595, L5

Nestor, D.B., Turnshek, D.A., & Rao, S.M. 2005, ApJ, 628, 637 (NTR05)

Nestor, D.B., Turnshek, D.A., & Rao, S.M. 2006, ApJ, 643, 75

Nestor, D.B., Turnshek, D.A., Rao, S.M., & Quider, A.M. 2007, ApJ, 658, 185

Nestor, D.B., Johnson, B.D., Wild, V., Ménard, B., Turnshek, D.A., Rao, S.M., & Pettini, M. 2011, MNRAS, in press (arXiv:1003.0693)

Norman, C.A., Bowen, D.V., Heckman, T., Blades, C., & Danly, L. 1996, ApJ, 472, 73

Phillips, S., Disney, M.J., & Davis, J.I. 1993, MNRAS, 260, 453

Prochter, G.E., Prochaska, J.X., & Burles, S.M. 2006, ApJ, 639, 766

Rao, S.M., Turnshek, D.A., & Briggs, F.H. 1995, ApJ, 449, 488

Rao, S.M., & Turnshek, D.A. 2000, ApJS, 130, 1

Rao, S.M., Nestor, D.B., Turnshek, D.A., Lane, W.M., Monier, E.M., & Bergeron, J. 2003, ApJ, 595, 94

Rao, S.M., Turnshek, D.A., & Nestor, D.B. 2006, ApJ, 636, 610

Rao, S. M., Belfort-Mihalyi, M., Turnshek, D. A., Monier, E. M., Nestor, D. B., & Quider, A. M. 2011, MNRAS, submitted

Rimoldini, L. 2007, PhD thesis (Univ. of Pittsburgh)

Sargent, W.L.W., Steidel, C.C., & Boksenberg, A. 1988, ApJ, 334, 22

Sargent, W.L.W., & Steidel, C.C. 1990, ApJ, 359, L37

Schneider, D.P., et al. 2007, AJ, 134, 102

Steidel, C.C., & Sargent, W.L.W. 1992, ApJS, 80, 1

Steidel, C.C., Dickinson, M., & Persson, S.E. 1994, ApJ, 437, L75

Steidel, C.C., Kollmeier, J.A., Shapley, A.E., Churchill, C.W., Dickinson, M., & Pettini, M. 2002, ApJ, 570, 526

Turnshek, D.A., Rao, S.M., Nestor, D.B., Belfort-Mihalyi, M., & Quider, A.M. 2005, in IAU Colloq. 199, Probing Galaxies Through Quasar Absorption Lines, ed. P. R. Williams, C.-G. Shu, & B. Ménard (Cambridge, Cambridge Univ. Press), 104, astro-ph/0506701

Tytler, D., Boksenberg, A., Sargent, W.L.W., Young, P., & Kunth, D. 1987, ApJS, 64, 667

Weymann, R.J., Williams, R.E., Peterson, B.M., & Turnshek, D.A. 1979, ApJ, 234, 33

York, D.G., et al. 2000, AJ, 120, 1579

Zibetti, S., Ménard, B., Nestor, D.B., & Turnshek, D.A. 2005, ApJ, 631, L105

Zibetti, S., Ménard, B., Nestor, D.B., Quider, A.M., Rao, S.M., & Turnshek, D.A. 2007, ApJ, 658, 161

This 2-column preprint was prepared with the AAS LaTeX macros v5.2.

Table 1: Metal-Line Measurements for J085244.74+343540.4 ($z_{em} = 1.655$)

Transition	λ_0 (Å)	$W_0^1 \pm \sigma_{W_0}$ (Å)
Mg II	2796.35	$3.046^2 \pm 0.083$
Mg II	2803.53	2.930 ± 0.085
Fe II	2586.65	1.567 ± 0.159
Fe II	2600.17	2.189 ± 0.166
Mn II	2576.88	1.261 ± 0.138
Mn II	2594.50	1.034 ± 0.179
Mn II	2606.46	0.583 ± 0.165
Mg I	2852.96	1.150 ± 0.087

[1] $z_{abs} = 1.3102$
[2] $W_0^{lim} = 0.372$ Å

Table 2: SDSS DR4 Quasars Searched for Mg II

Column	Description
1	J2000 name
2	SDSS Modified Julian Date (MJD)
3	SDSS Plate Number
4	SDSS Fiber Number
5	Right ascension (J2000)
6	Declination (J2000)
7	z_{em}
8	Error in z_{em}
9	BEST fiber u magnitude
10	BEST fiber g magnitude
11	BEST fiber r magnitude
12	BEST fiber i magnitude
13	BEST fiber z magnitude
14	Error in BEST fiber u magnitude
15	Error in BEST fiber g magnitude
16	Error in BEST fiber r magnitude
17	Error in BEST fiber i magnitude
18	Error in BEST fiber z magnitude